Condensation of Water Vapor in Rarefaction Waves: I. Homogeneous Nucleation

J. P. Sislian* and I. I. Glass†
University of Toronto, Toronto, Canada

A detailed theoretical investigation has been made of the condensation of water vapor/carrier gas mixtures in the nonstationary rarefaction wave generated in a shock tube. It is assumed that condensation takes place by homogeneous nucleation. The equations of motion together with the nucleation rate and the droplet growth equations were solved numerically by the method of characteristics and Lax's method of implicit artificial viscosity. It is found that, for the case considered, the condensation wave formed by the collapse of the metastable nonequilibrium state is followed by a shock wave generated by the intersection of characteristics of the same family. The expansion is practically isentropic up to the onset of condensation. The condensation front accelerates in the x,t plane. The results of the computations for a chosen case of water vapor/nitrogen mixture are presented by plotting variations of pressure, nucleation rate, number density of critical clusters, and condensate mass-fraction along three particle paths. Some consideration is given to homogeneous condensation experiments conducted in a shock tube. Although a direct comparison of the present theoretical work and these experiments is not possible, several worthwhile interpretative features have resulted nevertheless.

Introduction

IF the vapor of any substance is expanded isentropically and cooled, there is some time t at which the vapor becomes saturated. It is assumed that condensation then takes place in thermodynamic equilibrium. The fluid becomes a two-phase vapor-liquid system at t, and the vapor remains in equilibrium with the liquid at any subsequent time. In this case, the state of the fluid changes along the saturation curve. Many condensation processes in nature and technology follow equilibrium states closely, provided that liquid or solid-phase particles are present initially, which become condensation centers. However, in an ideally physically-pure gas, where significant foreign condensation nuclei are absent, centers of condensation must be created in the gas itself. In this situation, the condensation is said to take place by homogeneous nucleation and it may become much delayed with respect to the equilibrium states. The theory of the formation of nuclei of the liquid phase in a pure supersaturated vapor has been developed by a number of authors.[1] More recently, several authors[2] have tried to improve this classical theory by treating homogeneous nucleation from a statistical-mechanical viewpoint. Parallel to this work, extensive experimental and analytical investigations of condensation phenomena, primarily in steady supersonic nozzle flows, were carried on, both to check the validity of various available nucleation theories and to solve gasdynamic problems with condensation, of interest in different areas of engineering. Along with the techniques of steady nozzle flow, nonstationary condensation in a rarefaction wave produced in a shock tube provides one more possibility for the application of experimental and analytical methods to the resolution of fast processes.

Wegener and Lundquist[3] were the first to use the shock tube for condensation studies and the first streak photographs showing the condensation process in a rarefaction fan were obtained by Glass and Patterson.[4] More recently, several authors[5-10] have used the shock tube for the experimental investigation of the condensation of various vapors. In the present investigation, a detailed analytical study was made of the condensation of water vapor/carrier gas mixtures in the nonstationary rarefaction wave generated in a shock tube. Quantitative analytical and numerical methods were developed to predict the effects of nonequilibrium homogeneous condensation on the flow variables. The equilibrium condensation case to which the nonequilibrium flow tends asymptotically as $t \to \infty$ also has been determined.

Received Feb. 12, 1976; revision received June 7, 1976. The financial support received from the National Research Council of Canada, the Atomic Energy of Canada Ltd. (Chalk River) and the U.S. Air Force Office of Scientific Research (AF-AFOSR 72-2274) is acknowledged with thanks.

Index categories: Multiphase Flows; Nozzle and Channel Flow; Shock Waves and Detonations.

*Research Fellow, Institute for Aerospace Studies. Presently Research Associate, NASA Langley Research Center, Hypersonic Propulsion Branch.

†Professor, Institute for Aerospace Studies. Fellow AIAA.

Basic Equations

The problem to be considered in the present investigation is the following. A mixture of water vapor and an inert carrier gas at a given total pressure p_0 and temperature T_0 is initially at rest in the driver section of a shock tube. At time $t=0$, the diaphragm separating the driver section from the channel (low-pressure section) of the shock tube is removed, and the mixture suddenly is expanded into the channel. The vapor contained in the mixture is expanded isentropically by a rarefaction wave and cooled until it becomes saturated and as time increases it becomes supersaturated. Condensation then takes place by homogeneous nucleation and the droplets grow. The problem is to determine the effects of condensation on the nonstationary flowfield. The wave system following diaphragm rupture is illustrated in the time-distance (t,x) plane on Fig. 1. It can be seen that, in addition to the shock wave and rarefaction wave, a contact surface also forms, separating the original gases. Particle paths are shown also as well as the head and tail of the rarefaction wave.

In writing the basic equations, the following assumptions are made: 1) the effects due to viscosity and heat conduction are neglected; 2) up to the actual appearance of condensation, the gas mixture may be treated as a thermally and calorically perfect gas, i.e., the phase change occurs sufficiently far from the so-called critical point on the phase diagram; 3) the condensed mass is distributed uniformly throughout the gaseous components, and has the same velocity and temperature as the main flow; 4) the volume of the condensed phase is negligible compared to the total volume. The one-dimensional nonstationary flow of such a medium, with allowance for nonequilibrium homogeneous condensation, is described by

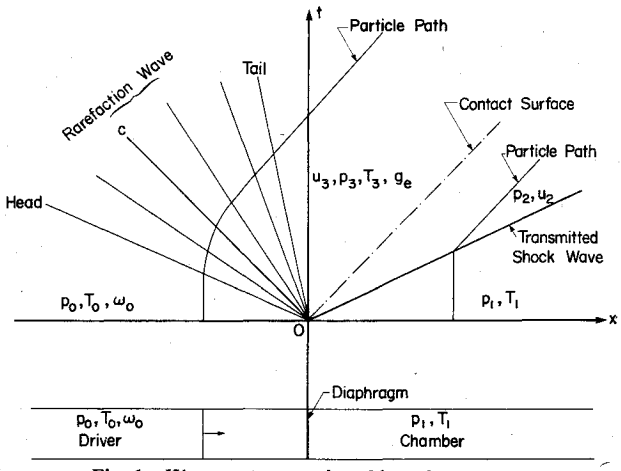

Fig. 1 Wave system produced in a shock tube.

the following equations:

Continuity

$$\frac{\partial \rho}{\partial t} + \frac{\partial (\rho u)}{\partial x} = 0 \tag{1}$$

Momentum

$$\frac{\partial u}{\partial t} + u\frac{\partial u}{\partial x} = -\frac{1}{\rho}\frac{\partial p}{\partial x} \tag{2}$$

Energy

$$\frac{\mathrm{d}h}{\mathrm{d}t} = \frac{1}{\rho}\frac{\mathrm{d}p}{\mathrm{d}t} \tag{3}$$

Rate equation

$$\frac{\mathrm{d}g}{\mathrm{d}t} = f(p, T, g) \tag{4}$$

Equation of state

$$p = \left(\frac{1-\omega_0}{\mu_i} + \frac{\omega_0}{\mu_v}\right)\rho RT \tag{5}$$

where t is time; x is the distance along the shock tube (Fig. 1); u and T are the velocity and temperature of the condensate and gas phase; p is the total pressure $p = p_i + p_v$ (i denotes the inert carrier gas, v the vapor); ρ is the total density ($\rho = \rho_i + \rho_v + \rho_c$, c denotes the condensate), g is the condensate mass fraction; $\omega_0 = m_{v_0}/m$ is the initial specific humidity; μ_i and μ_v are the molecular weights of the carrier gas and water vapor, respectively; and R is the universal gas constant. The expression for the specific enthalpy h of the two-phase mixture has the form[11]

$$h = c_{p_0} T - Lg \tag{6}$$

where the heat capacity at constant pressure c_{p_0} is given by

$$c_{p_0} = (1-\omega_0)c_{p_i} + \omega_0 c_{p_v} \tag{7}$$

and L is the latent heat of vaporization.

Equation (4) describes the "production" rate of the condensed phase along a particle path. The inception and growth of condensation nuclei, i.e., droplet nucleation and growth equations, as developed in Refs. 1, 11, and 12, are employed here.

The relationship between the vapor pressure p_v and the so-called critical radius r^* of a droplet in equilibrium with the vapor in which it is suspended is given by the Thomson equation[1]

$$r^* = \frac{2\sigma}{\rho_d (R/\mu_v) T \ln(p_v/p_s)} \tag{8}$$

where σ is the surface tension of the spherical droplet, ρ_d is its density, and p_s is the saturation pressure of the vapor phase. The equilibrium between the vapor and the critical droplet is unstable;[1] if $r > r^*$, the droplet grows; if $r < r^*$, it evaporates. Thus, there exists a minimum critical size which the droplet must have in order to become a condensation nucleus. The inception of the phase transition is determined by the probability of the generation of critical-size clusters. The number of critical-size droplets formed per unit time per unit volume, i.e., the nucleation rate, is given by[11]

$$I = \left(\frac{2}{\pi}\right)^{1/2} \frac{N_A^{3/2}}{R^2}\left(\frac{p_v}{T}\right)^2 \frac{(\sigma \mu_v)^{1/2}}{\rho_\ell} \exp\left(-\frac{4\pi r^{*2}\sigma}{3kT}\right) \tag{9}$$

where N_A is the Avogadro number, ρ_ℓ is the density of the condensing phase, and k is the Boltzmann constant.

Once a droplet is formed which is able to grow, its further growth is determined by a droplet-growth equation which expresses the mass increase of a critical-size droplet as it moves downstream with the flow. This equation includes the following further assumptions: 1) the droplets are spherical; 2) the droplet temperature is uniform; 3) each droplet grows separetely and does not coalesce with other droplets; 4) the mean free path in the gaseous medium is much longer than the droplet size; 5) the rate of droplet growth does not depend on its radius. Under these assumptions, it can be shown that the rate of droplet growth is given by[12]

$$\frac{\mathrm{d}r}{\mathrm{d}t} = \frac{\alpha}{\rho_\ell} \frac{p_s}{[2\pi(R/\mu_v)T]^{1/2}} (s-1) \tag{10}$$

where α is the so-called condensation coefficient (assumed constant) equal to the ratio of molecules sticking to the droplet to those impinging on it, and $s = p_v/p_s$ is the supersaturation.

The relative rate of formation of condensate along a particle path at time t may be derived as follows. A droplet of initial radius $r^*(\tau)$ formed at a certain instant τ along a particle path will grow to a size

$$r^*(\tau) + \int_\tau^t \frac{\mathrm{d}r}{\mathrm{d}t}\mathrm{d}\theta$$

at time t. The number of such nuclei formed at instant τ per unit mass per unit time is $I(\tau)/\rho(\tau)$. At instant t the rate of condensate accumulation on all these droplets is

$$\left\{\frac{I(\tau)}{\rho(\tau)}\rho_\ell \quad 4\pi\left[r^*(\tau) + \int_\tau^t \frac{\mathrm{d}r}{\mathrm{d}t}\mathrm{d}\theta\right]^2\right\}\frac{\mathrm{d}r}{\mathrm{d}t}\Bigg|_t$$

Integrating the above expression with respect to τ from the initial instant t_i to instant t along the particle path, and taking account also of the very small rate of condensation at t due to nucleation, the rate of production of the new phase is

$$\frac{\mathrm{d}g}{\mathrm{d}t} = 4\pi\rho_\ell\left\{\frac{I(t)}{\rho(t)}\frac{r^{*3}(t)}{3} + \frac{\mathrm{d}r}{\mathrm{d}t}\int_{t_i}^t \left[\frac{I(\tau)}{\rho(\tau)}\left(r^*(\tau) + \int_\tau^t \frac{\mathrm{d}r}{\mathrm{d}t}\mathrm{d}\theta\right)^2\right]\mathrm{d}\tau\right\} \equiv f \tag{11}$$

which represents the explicit form of Eq. (4). In this equation the quantities r^*, I, and $\mathrm{d}r/\mathrm{d}t$ are given by Eqs. (8), (9), and (10), respectively.

Numerical Solution and Results

Method of Characteristics

Equations (1-4) are not solvable analytically and we must resort to numerical methods of integration. For this, the hyperbolic character of these equations[13] may be used to reduce them to a system of equations of characteristics and the relationships on them, which describe the laws of propagation of disturbances in the nonstationary flowfield. The nondimensional variables and coordinates are

$$\bar{p}=\frac{p}{p_0},\ \bar{\rho}=\frac{\rho}{\rho_0},\ \bar{T}=\frac{T}{T_0},\ \bar{u}=\frac{u}{a_0},\ \bar{t}=\frac{t}{\tau},\ \bar{x}=\frac{x}{\ell} \tag{12}$$

where quantities with subscript 0 refer to the condition in the driver, a_0 is the speed of sound, ℓ and τ are some characteristic distance and time such that $\ell/\tau=a_0$. The complete set of characteristic equations in Eulerian coordinates in the $\bar{x}$, $\bar{t}$ plane is

$$\frac{d\bar{x}}{d\bar{t}}=\bar{u}\pm\bar{a}_f \tag{13}$$

$$\frac{d\bar{p}}{d\bar{t}}\pm\gamma_0\bar{\rho}\bar{a}_f\frac{d\bar{u}}{d\bar{t}}+\gamma_0\bar{\rho}\,\bar{a}_f^2\left(\frac{I}{(\mu_v/\mu_0)-g}-\frac{\lambda}{\bar{T}}\right)f_4=0 \tag{14}$$

$$\frac{d\bar{x}}{d\bar{t}}=\bar{u} \tag{15}$$

$$\frac{d\bar{C}}{d\bar{t}}=\frac{\bar{I}}{\bar{\rho}}\equiv f_1 \tag{16}$$

$$\frac{d\bar{B}}{d\bar{t}}=\frac{\bar{I}}{\bar{\rho}}\bar{r}^*+\dot{r}\,\bar{C}\equiv f_2 \tag{17}$$

$$\frac{d\bar{A}}{d\bar{t}}=\frac{\bar{I}}{\bar{\rho}}\bar{r}^{*2}+2\dot{r}\,\bar{B}\equiv f_3 \tag{18}$$

$$\frac{dg}{d\bar{t}}=4\pi\left(\frac{\bar{I}}{\bar{\rho}}\frac{\bar{r}^{*3}}{3}+\dot{r}\,\bar{A}\right)\equiv f_4 \tag{19}$$

$$d\bar{T}-\lambda\,dg-\frac{\gamma_0-1}{\gamma_0}\frac{d\bar{p}}{\bar{\rho}}=0 \tag{20}$$

where $\lambda=c_{p0}\,T_0/L$ and $\bar{a}_f$ is the nondimensional frozen speed of sound

$$\bar{a}_f^2\equiv\left(\frac{a_f}{a_0}\right)^2=\frac{\dfrac{\mu_v}{\mu_0}-g}{\dfrac{\mu_v}{\mu_0}-g+\gamma_0 g}\,\bar{T} \tag{21}$$

The upper signs in Eqs. (13) and (14) pertain to the right-running characteristics, and the lower signs to the left-running characteristics. Equations (15-19) hold along the particle path, Eq. (15), and are obtained from Eq. (11). Equation (20) is obtained from the energy equation [Eq. (3)] using Eq. (6). It can be seen that the characteristic sound speed in a condensing gas mixture is the frozen sound speed. This is similar to the case of a reacting gas mixture.[14]

Equations (13-20) were solved numerically by the second-order method suggested in Ref. 15, subject to initial conditions along the frozen rarefaction-wave head and at the center of the rarefaction wave. Computations by this method were performed only in the rarefaction fan of the flowfield where most of the spontaneous condensation occurs (see Fig. 2, region OBCDO). The numerical calculations were made using an IBM 370-165 at the Institute of Computer Science,

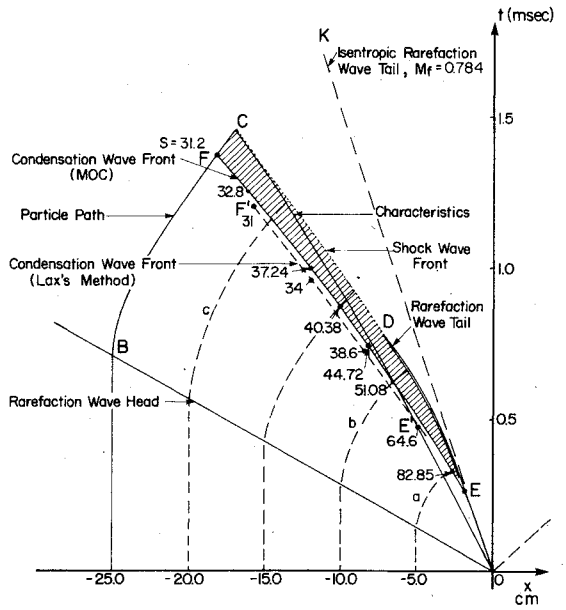

Fig. 2 Condensation-wave structure in nonstationary rarefaction wave.

University of Toronto, for the following initial conditions: nitrogen/water vapor mixture in the driver section characterized by the values $\omega_0=0.01776$, $\varphi_0=0.973$ (relative humidity of 97.3%), and $T_0=295.3°K$. The low-pressure chamber contained air at $T_1=T_0$. The diaphragm pressure ratio was 6.8. The details of the computation are given in Ref. 16.

A sketch of the predicted flowfield in the physical x,t plane is shown in Fig. 2. The line OB is the head of the rarefaction wave moving at the rest state sound speed into the gas (as no condensation occurs there) with a velocity $a_0=352.2$ m/sec. The frozen (isentropic) tail of the wave is shown by the dashed line OK, and corresponds to a frozen Mach number $M_{f0}=0.784$, for a diaphragm pressure ratio of 6.8. The line EF representing the leading front of the condensation wave, i.e., the onset of condensation, obtained by the method of characteristics, is defined as the locus of points along particle paths where the supersaturation reaches its maximum value. Some of these values are shown along the condensation front. It is seen readily that the flow of a condensing mixture of water vapor/carrier gas with fixed initial relative humidity, experiences decreasing supercooling or supersaturation s with time and the leading front of condensation accelerates in the x,t plane. The hatched region represents the condensation zone within the rarefaction wave. It is the region of the flow where the collapse of the metastable state of the gas mixture occurs. The sudden precipitation of moisture affects the flow variables appreciably because of the sudden heat release by condensation (see Fig. 3). The characteristics emanating from point O remain straight as long as the effect of homogeneous condensation on the flow variables is negligibly small. After penetrating the condensation zone, the characteristics begin to curve appreciably towards the head of the rarefaction wave because of the latent heat of condensation. A typical characteristic OC is shown in Fig. 2.

Computations show that, for the case considered, the condensation wave is followed by a shock wave DC (Fig. 2) generated by the intersection of characteristics of the same family, i.e., the left-running characteristics. Within the boundaries of the computed flow region and the limitations of a finite characteristic mesh size, the line DC represents approximately the locus of intersection points of left-running characteristics which is the envelope of the shock wave. It is seen that the tail of the rarefaction wave is strongly curved, line OED, and the shock wave starts at point D. The

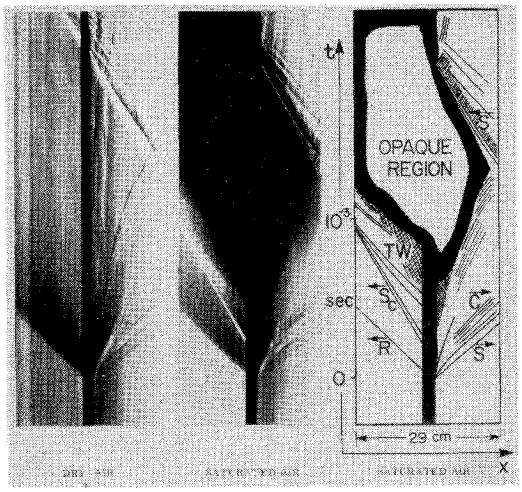

Fig. 3 Time-distance (t,x) schlieren photograph of the shock-tube problem near the origin with dry air and saturated air as driver gases. The head of the rarefaction wave ($\bar{R}$), the condensation shock wave ($\bar{S}_c$), the condensation region, the contact surface ($\bar{C}$), the shock wave ($\bar{S}$), and transverse waves from the diaphragm breaking process (TW), are shown clearly in the saturated air case. Initial conditions: $P_4 = 746$ Torr, $p_1 = 29.8$ Torr $T_4 = 297°$K, $T_1 = 297°$K, $\varphi_4 = 100\%$, $\omega_4 = 1.8\%$ (calculated) (Refs. 4, 22).

possibility of the occurrence of discontinuities during homogeneous condensation already has been noted by several authors.[17-21] The present analysis establishes the occurrence of such discontinuities during the homogeneous water-vapor condensation in a nonstationary rarefaction wave for the initial conditions considered.

The occurrence of shock waves during homogeneous condensation of water vapor in a nonstationary rarefaction wave in a shock tube has been established also experimentally by Glass et al.[22] Figure 3 shows an x,t schlieren photograph of the condensation region for water vapor condensation in air in a shock tube in the region of the diaphragm. The experimental initial conditions are given in the figure. The calculated initial relative humidity and specific humidity were found to be $\varphi_0 = 100\%$ and $\omega_0 = 1.8\%$, respectively. These initial values are close to the case considered in the present investigation. The condensation shock wave S_c is seen readily in the photograph. However, no curvature was observed in the experimental path of this shock. It is of interest to note the resemblance of the shock found for the present case of phase change in a nonstationary rarefaction wave, with the recombination shock in a relaxing gas predicted by Glass and Takano[23] in a corner-expansion type flow, where in a dissociated gas, energy (heat) is transferred from the internal degrees to the active degrees of freedom during recombination.

The width of the condensation wave increases with increasing distance from the origin (hatched area in Fig. 2) because of the interplay of two varying opposing effects, namely, the variable rates of expansion, which decrease the pressure, and of heat addition due to condensation in the nonstationary subsonic flow, which increases the pressure. Closer to the origin where conditions are nearly frozen, the expansion rate is very high, whereas the rate of condensation varies less markedly. For this reason the condensation front in the rarefaction fan starts at some distance from the origin at point E on the tail of the wave. At point E the condensation front is about 2 cm thick.

Lax Method

The presence of shock waves in the flowfield complicates the solution of the problem. In order to handle such discontinuities in the flowfield, Lax's method of implicit artificial viscosity was used in the present investigation. This technique requires that all partial differential equations of motion be in conservative Lagrangian form. In nondimensional variables and coordinates [see Eq. (12)] they are

Continuity

$$\frac{\partial \bar{v}}{\partial \bar{t}} = \frac{\partial \bar{u}}{\partial \bar{y}} \tag{22}$$

Momentum

$$\frac{\partial \bar{u}}{\partial \bar{t}} = \frac{\partial(-\bar{p}/\gamma_0)}{\partial \bar{y}} \tag{23}$$

Energy

$$\frac{\partial \bar{E}}{\partial \bar{t}} = \frac{\partial(-\bar{p}\bar{u}/\gamma_0)}{\partial \bar{y}} \tag{24}$$

where $\bar{v} = 1/\bar{\rho}$, $\bar{E} = \bar{e} + \bar{u}^2/2$, and $\bar{y}$ is the nondimensional Lagrangian coordinate. Together with the rate equations [Eqs. (16-19)] written in Lagrangian form (the time derivative along a particle path is replaced by the partial time derivative $\partial/\partial \bar{t}$), the equation of state, Eq. (5), and the expression

$$\bar{T} = \frac{\gamma_0(\gamma_0 - 1)(\bar{E} - \bar{u}^2/2) + \gamma_0 \lambda g}{1 + (\gamma_0 - 1)(\mu_0/\mu_v)g} \tag{25}$$

for the specific internal energy for the mixture of gases and condensate, they form a determined system of equations. Lax approximates Eqs. (22-24) by the following difference scheme of first-order accuracy

$$\frac{1}{\Delta \bar{t}}(q_j^{n+1} - q_j^n) = \frac{1}{2\Delta \bar{y}}(W_{j+1}^n - W_{j-1}^n)$$

$$+ \frac{\mu}{\Delta \bar{t}}(q_{j+1}^n - 2q_j^n + q_{j-1}^n) \tag{26}$$

where $q = (\bar{v}, \bar{u}, \bar{E})$, $W = (\bar{u}, -\bar{p}/\gamma_0, -\bar{p}\bar{u}/\gamma_0)$, and μ is a constant; q_j^n is the value of q at the point $(j\Delta \bar{y}, n\Delta \bar{t})$ in the space-time network. The rate equations, Eqs. (16-19), which are of the general form,

$$\partial c_i/\partial \bar{t} = \bar{f}_i(\bar{v}, \bar{T}, c_k), \quad i, k = 1, \ldots, 4 \tag{27}$$

were integrated using a first-order implicit integration scheme[24]

$$c_{i,j}^{n+1} = c_{i,j}^n + \mu(c_{i,j+1}^n - 2c_{i,j}^n + c_{i,j-1}^n) + \{\bar{f}_i(\bar{v}_j^{n+1}, T_j^n, c_{k,j}^n)$$

$$+ \sum_{k=1}^{4} \frac{\partial \bar{f}_i}{\partial c_k} \Big|_j^n (c_{k,j}^{n+1} - c_{k,j}^n) + \frac{\partial \bar{f}_i}{\partial \bar{T}} \Big|_j^n (\bar{T}_j^{n+1} - \bar{T}_j^n)\} \Delta \bar{t} \tag{28}$$

Together with Eq. (25) written in differential form they form a system of five algebraic equations for the five unknowns $c_{i,j}^{n+1}$ T_j^{n+1}. Implicit integration methods were shown to be inherently stable in integrating the rate equations in all flow situations (whether near equilibrium, nonequilibrium, or frozen).[24] The time increment $\Delta \bar{t}$ is determined from the Courant stability condition

$$\Delta \bar{t} = \xi(\Delta \bar{y}/(\bar{\rho}\bar{a}_f)_{\max}^n \tag{29}$$

where ξ is a constant less or equal to unity. In Eulerian coordinates the computed flowfield is limited by time levels $t = 0$ and $t = \tau$ (the characteristic time), by a wall at a distance $\ell = a_0\tau$ from the diaphragm and the contact surface, which travels at a speed corresponding to the frozen state at point O (Fig. 2) for the given pressure ratio across the diaphragm.[16] Right and left boundary points were handled using the reflec-

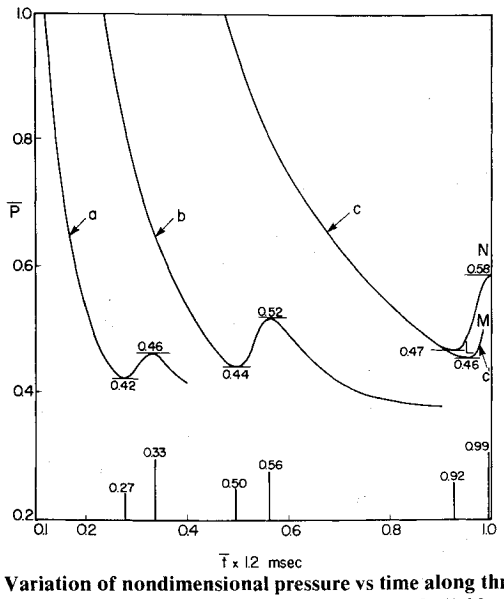

Fig. 4 Variation of nondimensional pressure vs time along three particle paths initially at: a) 5 cm, b) 10 cm, c) 20 cm, and c′) 20 cm from the diaphragm (*MOC*).

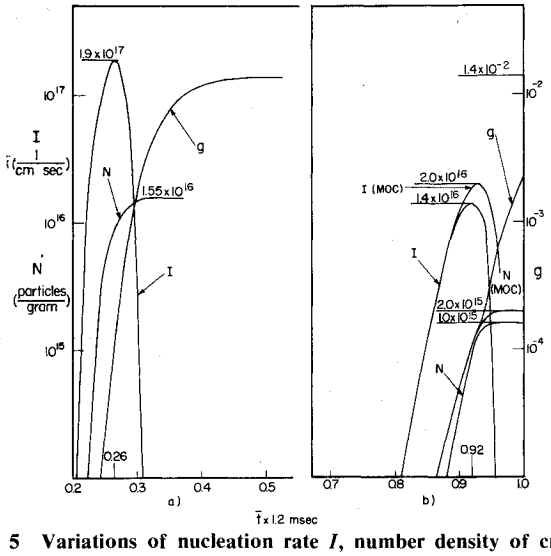

Fig. 5 Variations of nucleation rate I, number density of critical clusters N and condensate mass fraction g vs time along two particle paths initially at: a) 5 cm and b) 20 cm from the diaphragm.

tion technique.[25] The numerical calculations for the case considered in the present investigation were performed by the previously described Lax's method for $\xi = 0.75$, $\mu = 0.2$, on an IBM 370-165.[16]

The dashed line $E'F'$ in Fig. 2 is a portion of the onset of condensation calculated by Lax's method. The agreement with the results given by the method of characteristics, line EF, is satisfactory. The maximum supersaturations at the onset obtained by the two methods agree well far from the origin, where the rates of expansion computed by Lax's method agree closely with that given by the exact solution. Closer to the origin this agreement deteriorates, especially near the tail of the rarefaction wave where the onset of condensation occurs, and the supersaturations at the onset given by the two methods differ markedly in this region. Variations of the nondimensional pressure along three particle paths are shown in Fig. 4 (curve c' is the solution given by the method of characteristics). It readily is seen that the pressure rises due to homogeneous condensation are higher for particle paths farther from the origin (Fig. 2). The strength of the condensation wave along the particle path c (or c') due to the pressure increase from point L to M is $p_M/p_L = 1.073$, whereas the condensation shock from M to N has a strength $p_N/p_M \approx 1.19$. All curves tend asymptotically, for $t \to \infty$, to their common constant equilibrium value[16] of $\bar{p} \sim 0.39$ (see Fig. 4).

Figure 5 shows the variations along two particle paths of the rate of formation of condensation nuclei I, nuclei population N, and the condensate mass fraction g. The rate of formation of critical-size nuclei increases rapidly attaining values as high as $I = 1.9 \times 10^{17}$ particles/cm^3 sec on particle path a, and then upon partial reduction in supersaturation due to precipitation of moisture, it drops even more rapidly to zero as the curve is asymmetric with respect to the maximum. The total number of nuclei during the initial phase of homogeneous condensation also increases rapidly and approaches a value of 1.55×10^{16} particles/g on particle path a, and after the complete collapse of the supersaturated state remains constant. Because of the rapid nucleation process just before the onset of condensation the condensate mass fraction increases sharply. Further accumulation of condensate occurs mainly by accretion of vapor on critical droplets. All curves for the condensate mass fraction tend to their equilibrium value $g_e \sim 1.4 \times 10^{-2}$ in the quasi constant region of flow, downstream of the condensation zone.

Comparisons with Experimental Data

An experimental investigation of homogeneous condensation of water vapor in a nonstationary expansion of a water vapor/nitrogen (ultra pure N_2) mixture in a shock tube (2.54-cm × 2.54-cm cross section) was performed.[10] The density and pressure variations as well as the onset of condensation were monitored at two fixed locations in the driver section. An examination of the experimental pressure profile obtained for the case considered in the present investigation, at a location $x = -17.1$ cm from the diaphragm, shows that the experimental rate of expansion is markedly lower than the theoretical one at that location. It was found that the experimentally measured expansion rate at the head of the rarefaction wave corresponds more to the theoretical one at a distance $x = -23.4$ cm from the diaphragm. Although the agreement between theoretical and experimental isentropic (frozen) expansion rates is, in general, good (Fig. 6), it readily is seen and it may be shown, using the approach developed in Ref. 26, that the experimental waveform is noncentered. The homogeneous condensation process is very sensitive to the rates of expansion and cooling. The degree of supercooling increases rapidly with an increasing rate of expansion. This fact should be kept in mind when comparing the analytical results, based on the theory of ideal shock-tube flow, where it is

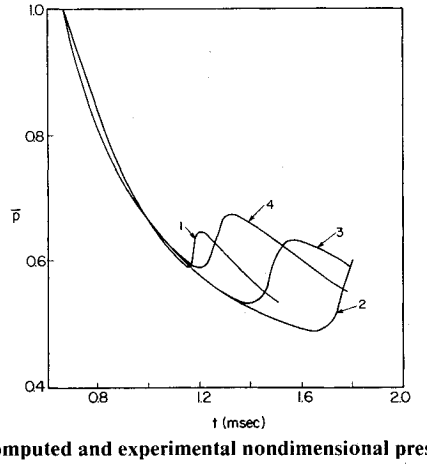

Fig. 6 Computed and experimental nondimensional pressure vs time at station $x = -23.4$ cm from the diaphragm: 1) experimental (Kalra[10]), $s_{onset} = 13.75$; 2) computed, $\sigma = 82$ dyn/cm, $s_{onset} = 25.8$; 3) computed, $\sigma = 75.6$ dyn/cm, $s_{onset} = 16.75$; 4) computed, $\sigma = 68.0$ dyn/cm, $s_{onset} = 10.4$.

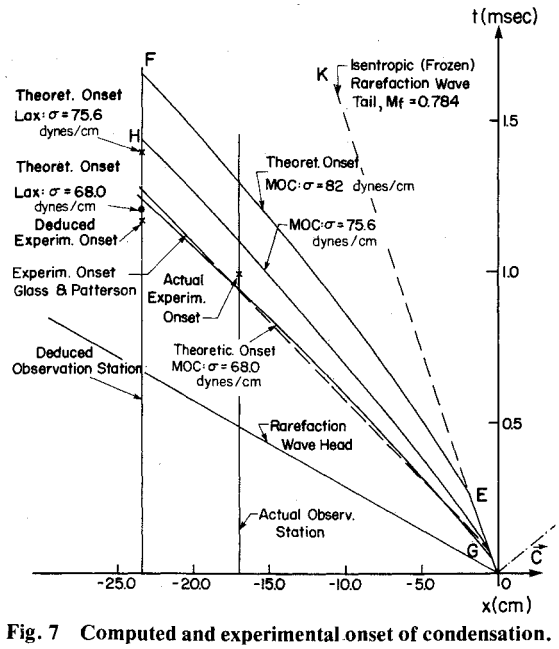

Fig. 7 Computed and experimental onset of condensation.

assumed that the nonstationary rarefaction wave generated by diaphragm rupture is a perfectly centered planar wave, with data obtained from experiments in which the waveforms not only are noncentered but also may be nonplanar at distances relatively close to the diaphragm. Nevertheless, the theoretical pressure variations were compared with the experimental profile at this modified location (Fig. 6).

Another point to be mentioned concerns the interfacial tension σ, i.e., the surface tension of the liquid droplet or the surface free-energy of an ice cluster. This physical quantity enters Eq. (9) for the nucleation rate in the exponential term to the third power, and therefore its correct value is the most critical aspect of the theoretical prediction of the condensation phenomenon. The major uncertainties are: 1) the possible effect of droplet size on the values of σ and 2) the choice between surface tension of a liquid droplet and surface free-energy of ice crystals, as the nature of the condensate is not precisely known. For a condensation coefficient value of $\alpha = 0.04$ considered throughout the present computations, the nondimensional pressure variation calculated at $x = -23.4$ cm is shown (curve 2) in Fig. 6, and the onset of condensation is depicted in Fig. 7 by curve *EF*. The semiempirical expression used for the surface tension[12] was $\sigma = 128 - 0.192T°K$ dyn/cm, and assuming the condensate to be liquid, this gives at the onset of condensation a value $\sigma = 82$ dyn/cm. The discrepancy with the experimental data is quite appreciable. For a constant surface tension value of $\sigma = 75.6$ dyn/cm suggested by Wegener[11] for water vapor/carrier gas condensation, the onset of condensation (line *GH* in Fig. 7) and the pressure variation (curve 3 in Fig. 6) are closer to those experimentally predicted. Good agreement with experiments performed at the University of Toronto Institute for Aerospace Studies, concerning the onset of condensation, is reached for $\sigma = 68.0$ dyn/cm as shown by curve 4 in Fig. 6 and in Fig. 7.

It is not very satisfactory to fit experimental data by altering physical parameters like σ.[27] It points to the fact that we do not have verified data for droplets at such conditions. There is considerable uncertainty in choosing a suitable value for the condensation coefficient α. The growth-law, Eq. (10), is applied without knowing whether the condensate is in liquid or solid form. The value $\alpha = 0.04$ chosen in the present computations and suggested by several authors[12] seems to be somewhat high for the case considered. Yet some authors believe it should approach unity.[28] The error in the absolute pressure rise is 30% and in the strength of the condensation shock wave ~ 12% for curve 4 (Fig. 6).

As noted previously, the initial conditions in the driver section of the shock tube in the experiments of Glass et al.[22] are close to those considered in the present investigation. Despite the fact that the wave system near the origin is not ideal and hence the rarefaction wave is neither centered nor planar, the experimental condensation shock wave path (Fig. 3), which has a uniform velocity of 190.5 m/sec lies just behind the onset of the condensation path as predicted for $\sigma = 68.0$ dyn/cm and $\alpha = 0.04$ (Fig. 7), and is in very reasonable agreement with the present calculations for Kalra's experiment.[10] It should be noted that this line was drawn from point *G* and with the measured slope from Fig. 3. The point *G* does not vary much with changes in σ.

Another feature is observed in Fig. 3, namely, the opaque region. From the analysis, most of the condensation occurs beyond the condensation front and condensation shock wave, (Fig. 5) and soon approaches a constant equilibrium value. Consequently, it is possible for the droplets, either in liquid or solid form (both have nearly the same refractive index), to grow and completely scatter and refract the schlieren beam to make it appear as an opaque region. Unfortunately, droplet size and film opacity were not measured as a function of time in the original experiments conducted over two decades ago. It is worth noting that Smith did observe a concave condensation front in steady corner-expansion waves,[29] and that a similar type of analysis for nozzle flows with condensation has appeared in Ref. 30.

Conclusions

An analytical and numerical analysis has been made of the condensation of water vapor/carrier gas mixtures in the rarefaction wave generated in a shock tube. Comparisons with experiments show that Frenkel's theory[1] appears to provide a good approximation for the rate of formation of condensate. The solution follows the isentrope to the point of condensation and then rapidly approaches the equilibrium condensation. The head of the condensation wave (the line of onset of condensation) is found to accelerate in the x,t plane. One of the most important results obtained for the case considered is that the condensation wave is followed by a shock wave generated by the intersection of characteristics of the same family. The critical droplet radius is computed to be of the order of 10^{-8} cm and grows to a maximum of $\sim 10^{-6}$ cm. These values are consistent with the assumptions made in the theory. In comparing the analytical results based on the theory of ideal shock-tube flow, where it is assumed that the nonstationary rarefaction wave generated by diaphragm rupture is a perfectly centered planar wave, to data obtained from experiments, it should be kept in mind that experimental waveforms are not only noncentered but also may be nonplanar with appreciable differences between theoretical and experimental rates of expansion and cooling. In addition, the values of surface tension σ, and the condensation coefficient α, are not known with any precision. In view of this, the agreement of analysis and experiment may be considered as quite satisfactory. The present analysis can be used in the future should new developments occur in the droplet growth or rate equations and it also can be applied to other problems in gasdynamics. It will be shown in a forthcoming paper that the experimental results considered in this publication also can be explained well using a heterogeneous nucleation model. In that model, the droplet contact angle with the surface of the nucleus (which is not known experimentally) plays the dominant role, just as σ does in homogeneous nucleation.

References

[1] Frenkel, J., *Kinetic Theory of Liquids*, Oxford University Press, New York, 1946.

[2] Dunning, W. J., "General and Theoretical Introduction," *Nucleation*, edited by A. C. Zettlemoyer, Marcel Dekker, Inc., New York, 1969, Ch. 1, pp. 3-67.

[3] Wegener, P. P. and Lundquist, G., "Condensation of Water Vapor in the Shock Tube Below 150°K," *Journal of Applied Physics*, Vol. 22, Feb. 1951, p. 233.

[4] Glass, I. I. and Patterson, G. N., "A Theoretical and Experimental Study of Shock-Tube Flows," *Journal of the Aeronautical Sciences*, Vol. 22, Feb. 1955, pp. 73-100.

[5] Courtney, W. G., "Condensation in a Rarefaction Wave," TR Suppl. No. 2, ONR NR 092 517/4-29-65, Dec. 1965, Office of Naval Research, Thiokol Chemical Corporation, Denville, N.J.

[6] Homer, J. B., "Studies on the Nucleation and Growth of Metallic Particles from Supersaturated Vapors," *Shock Tube Research, Proceedings of the Eighth International Shock Tube Symposium*, edited by J. L. Stollery, A. G. Gaydon, and P. R. Owen, Chapman and Hall, London, 1971.

[7] Kung, R. T. V. and Bauer, S. H., "Nucleation Rates in Fe Vapor: Condensation to Liquid in Shock Tube Flow," *Shock Tube Research, Proceedings of the Eighth International Shock Tube Symposium*, edited by J. L. Stollery, A. G. Gaydon, and P. R. Ownn, Chapman and Hall, London, 1971.

[8] Barschdorff, D., "Carrier Gas Effects on Homogeneous Nucleation of Water Vapor in a Shock Tube," *The Physics of Fluids*, Vol. 18, May 1975, pp. 529-535.

[9] Kawada, H. and Mori, Y., "A Shock Tube Study on Condensation Kinetics," *Nihon Kikaigakkai, Bulletin of Japanese Society of Mechanical Engineers*, Vol. 16, July 1973, pp. 1053-1065.

[10] Kalra, S. P., "Experiments on Nonequilibrium, Nonstationary Expansion of Water Vapor/Carrier Gas Mixture in a Shock Tube," Rept. No. 195, April 1975, University of Toronto, Institute for Aerospace Stuies.

[11] Wegener, P. P., "Gasdynamics of Expansion Flows with Condensation and Homogeneous Nucleation of Water Vapor," *Nonequilibrium Flows,* edited by P. P. Wegener, Marcel Dekker, Inc., New York, 1970, Ch. 4, Pt. 1.

[12] Hill, P. G., "Condensation of Water Vapor during Supersonic Expansion in Nozzles," *Journal of Fluid Mechanics*, Vol. 25, 1966, pp. 593-620.

[13] Courant, R. and Friedrichs, K. O., *Supersonic Flow and Shock Waves*, Interscience Publishers Inc., New York, 1948.

[14] Chu, B. T., "Wave Propagation and the Method of Characteristics in Reacting Gas Mixtures with Applications to Hypersonic Flow," TN-57-213, May 1957, Wright Air Development Center, Division of Engineering, Brown University, Providence, R.I.

[15] Kliegel, J. R., Peters, R. L., and Lee, J. T., "Characteristics Solutions for Nonequilibrium Flow Fields about Axisymmetric Bodies," Vol. II, Computer Program, TRW Rept. 6453-6001-Ku-000, 1964, Redondo Beach, Calif.

[16] Sislian, J. P., "Condensation of Water Vapor with or without a Carrier Gas in a Shock Tube," Rept. No. 201, Nov. 1975, University of Toronto, Institute for Aerospace Studies.

[17] Hermann, R., "Condensation Shock Waves in Supersonic Wind Tunnel Nozzles," *Luftfahrtforschung*, Vol. 19, June 1942, pp. 201-209.

[18] Oswatitsch, K., "Kondensationserscheinungen in Uberschalldusen," *Zeitschrift für Angewandte Mathematik und Mechanik,* Vol. 22, 1942, p. 1; translated by British Ministry of Aircraft Production as R.T.P. No. 1905.

[19] Heybey, W. H., "Analytical Treatment of Normal Condensation Shock," NACA Technical Memo, 1174, 1947.

[20] Pouring, A. A., "Thermal Choking and Condensation in Nozzles," *The Physics of Fluids*, Vol. 8, Oct. 1965, pp. 1802-1810.

[21] Bartlma, F., "Ebene Uberschallstromung mit relaxation," *Proceedings of 11th Congress of Applied Mechanics*, 1964, Munich,

[22] Glass, I. I., Martin, W. A., and Patterson, G. N., "A Theoretical and Experimental Study of the Shock Tube," Rept. No. 2, Nov. 1953, University of Toronto Institute for Aerospace Studies, Toronto, Canada.

[23] Glass, I. I. and Takano, A., "Nonequilibrium Expansion Flows of Dissociated Oxygen and Ionized Argon Around a Corner," *Progress in Aeronautical Sciences*, Vol. 6, edited by Kuchemann and Sterne, Pergamon Press, Oxford, 1965, pp. 163-249.

[24] Katskova, O. N. and Kraiko, A. N., "Calculation of Plane and Axisymmetric Supersonic Flows with Irreversible Processes," *Zhurnal Prikladnoi Makhaniki I Tekhnicheskoi Fiziki*, No. 4, 1963, pp. 116-118.

[25] Roache, P. J., *Computational Fluid Dynamics*, Hermosa Publishers, Albuquerque, N.M., 1972.

[26] Hall, J. G., Srinivasan, G., and Rathi, J. S., "Unsteady Expansion Waveforms Generated by Diaphragm Rupture," *AIAA Journal*, Vol. 12, May 1974, pp. 724-726.

[27] Wegener, P. P., Clumpner, J. A., and Wu, B. J. C., "Homogeneous Nucleation and Growth of Ethanol Drops in Supersonic Flow," *The Physics of Fluids*, Vol. 15, Nov. 1972, pp. 1869-1876.

[28] Mills, A. F. and Seban, R. A., "The Condensation Coefficient of Water," *International Journal of Heat and Mass Transfer*, Vol. 10, 1967, pp. 1815-1827.

[29] Smith, L. T., "Experimental Investigation of the Expansion of Moist Air Around a Sharp Corner," *AIAA Journal*, Vol. 9, Oct. 1971, pp. 2035-2037.

[30] Bratos, M. and Jaeschke, M., "Two-Dimensional Flows with Non-Equilibrium Phase Transitions," Rept. No. 648/0/74, W-108, 1974, Instytut Podstawowych Problemow Techniki, PAN, Warsaw, Poland.